Full Paper Transactions, SMiRT 28
Toronto, Canada, August 10-15, 2025

SMATCH BENCHMARK: SEISMIC RESPONSE ANALYSIS OF THE BASE-ISOLATED CRUAS NPP SUBJECTED TO THE LE-TEIL EARTHQUAKE USING THE ANSYS APDL SOFTWARE

Eleni Eleftheriou[1], Jan Attinger[2], Peter Rangelow[3], Sara Ghadimi Khasraghy[4], Tadeusz Szczesiak[5]

[1] Structural Engineer, Basler & Hofmann AG, Zurich, Switzerland (eleni.eleftheriou@baslerhofmann.ch)
[2] Project Manager, Basler & Hofmann AG, Zurich, Switzerland (jan.attinger@baslerhofmann.ch)
[3] Dr., Senior Expert, Basler & Hofmann AG Consulting Engineers, Zurich, Switzerland (peter.rangelow@baslerhofmann.ch)
[4] Dr., Civil Engineering Specialist, Swiss Federal Nuclear Safety Inspectorate ENSI, Brugg, Switzerland (sara.ghadimi@ensi.ch)
[5] Dr., Deputy Section Head of Civil Engineering, Swiss Federal Nuclear Safety Inspectorate ENSI, Brugg, Switzerland (tadeusz.szczesiak@ensi.ch)

ABSTRACT

The Cruas Nuclear Power Plant (NPP) is a Pressurised Water Reactor (PWR) located in France and built on a seismic base isolation using laminated steel-neoprene bearings. The “Le Teil” earthquake occurred at approximately 15 km from the Cruas NPP on November 11, 2019, and resulted in a Peak Ground Acceleration (PGA) between 0.02 and 0.05 g in the free field (Viallet et al., 2022). The ground and in-structure responses of the Nuclear Island (NI) were recorded during the earthquake, in accordance with operational procedures. In this context, the international benchmark SMATCH was organised by IRSN (Institut de Radioprotection et de Sûreté Nucléaire) and EDF (Électricité de France), under the auspices of the OECD Nuclear Energy Agency (NEA), with the objective of exploiting the recorded data and improving the scientific and engineering understanding of the effect of real earthquakes on seismically isolated facilities. The Swiss Federal Nuclear Safety Inspectorate (ENSI) supports three teams participating in Phase 3 of this benchmark, which aims at predicting the seismic behaviour of the NPP. In this paper the results of the team ‘ENSI-Basler & Hofmann AG’ are presented.

This paper reports on the modelling and the seismic response analysis of the base-isolated Cruas NPP subjected to the Le-Teil earthquake. It discusses the influence of the bearing characteristics and highlights the challenges in modelling and calculation of seismically isolated structures. The analysis is performed using the finite element (FE) software ANSYS 2021 R2 (APDL), in which the bearings are modelled with global springs acting in the horizontal and vertical directions. For the buildings of the nuclear island stick-models consisting of Timoshenko-beam elements have been used. Shell elements are used to model the foundation raft. The analysis demonstrates that this simplified modelling approach effectively captures the global response of the NI, while allowing a significant reduction of the calculation time. The nonlinear behaviour of the bearings appears to play a crucial role even for small earthquake-induced displacements, necessitating appropriate constitutive modelling. Given the good fit of the calculated and recorded accelerations, detailed soil-structure interaction modelling appears to be less critical for the global horizontal response of base-isolated structures. However, this may not be generalisable to all site conditions and isolation device configurations.

INTRODUCTION

During the Le Teil earthquake, with a magnitude of 4.9 (Mw), acceleration-time histories were recorded in the free-field and at sensor locations within the Cruas NPP building, located about 15 km from the epicentre.

The nuclear island of the Cruas NPP is seismically base-isolated (Figure 1), with the buildings supported by a shared upper raft foundation. This upper raft is supported by 1812 laminated elastomeric bearings, which are grouped in sets of two, four, or eight based on load distribution requirements. These bearings are mounted on 401 reinforced concrete pedestals, which transfer loads to a lower raft foundation on the ground.

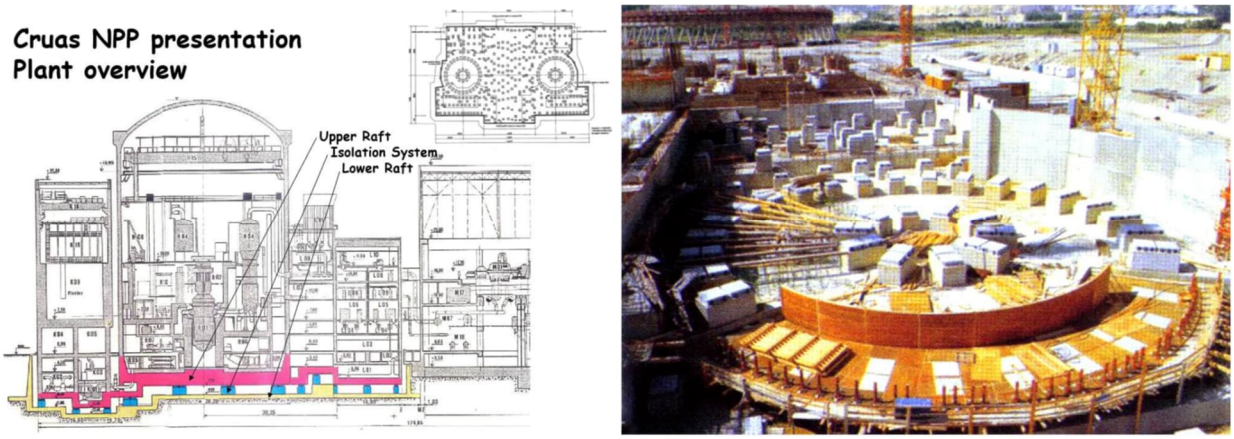

Figure 1. Seismic base isolation of the Cruas NPP (Viallet et al., 2022, EDF/IRSN/Egis): (left) structural layout; (right) construction-phase photo showing the pedestals designed to support the seismic bearings

The SMATCH benchmark aims to enhance the understanding of seismic behaviour at location of the Cruas NPP by simulating the seismic motion induced by the Le Teil earthquake (Phase 2) and analysing the structural response of the NPP (Phase 3). This paper focuses on Phase 3, which consists of:

- Phase 3.1: Blind prediction of the structural response, based on predefined input conditions;
- Phase 3.2: Calibration of numerical results using recorded seismic data.

The study evaluates key dynamic response parameters, including acceleration-time histories, In-Structure Response Spectra (ISRS), transfer functions, and time-frequency Stockwell wavelet transform (ST) plots. These outputs are analysed at three key sensor locations (Figure 2) within the reactor and auxiliary buildings:

- EAU 001 (Reactor Building, elevation -3.40 m);
- EAU 002 (Reactor Building, elevation +19.15 m);
- EAU 003 (Auxiliary Building, elevation -0.90 m).

The benchmark organisers provided specific data, including the structural model of the Cruas NPP, the elastomeric bearing properties, and the results of the modal analysis of the structure.

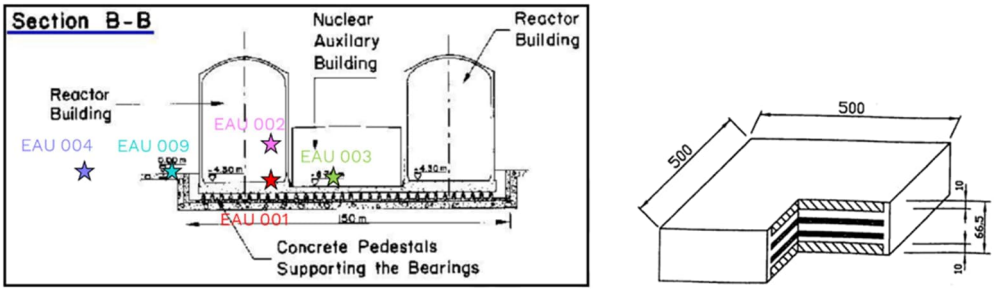

Figure 2. (left) Location of the EAU seismic sensors within the reactor and auxiliary buildings of the CRUAS NPP; (right) exemplary drawing of a laminated steel-neoprene bearing; (Viallet et al., 2022, EDF/IRSN/Egis)

FINITE ELEMENT MODEL OF THE CRUAS NPP NUCLEAR ISLAND

A simplified computational model of the NI of the Cruas NPP is developed in the FE simulation software ANSYS, where the foundation slab above the seismic isolation is modelled as a shell structure and all buildings are represented as stick models. The stick models of all the buildings (Figure 3), except for the auxiliary building, are directly converted from the benchmark-provided stick models into ANSYS APDL. The auxiliary building is modelled as a single-degree-of-freedom (SDOF) oscillator, despite the availability of a more detailed shell model. The upper raft foundation is modelled as a rigid body. Under each building, springs represent the stiffness and damping characteristics of the seismic isolation bearings. These springs allow for a simplified simulation of the bearing behaviour in the x, y, and z directions.

The Foundation Input Motion (FIM), determined using SASSI by the ENSI-Team SPI (to be presented in a separate paper at SMiRT-28), is applied at the lower ends of the springs. No additional springs or elements are included to represent the impedance of the soil layers beneath the foundation. Consequently, the model neglects inertial soil-structure interaction effects and focuses solely on the structural response and dynamic behaviour of the bearings.

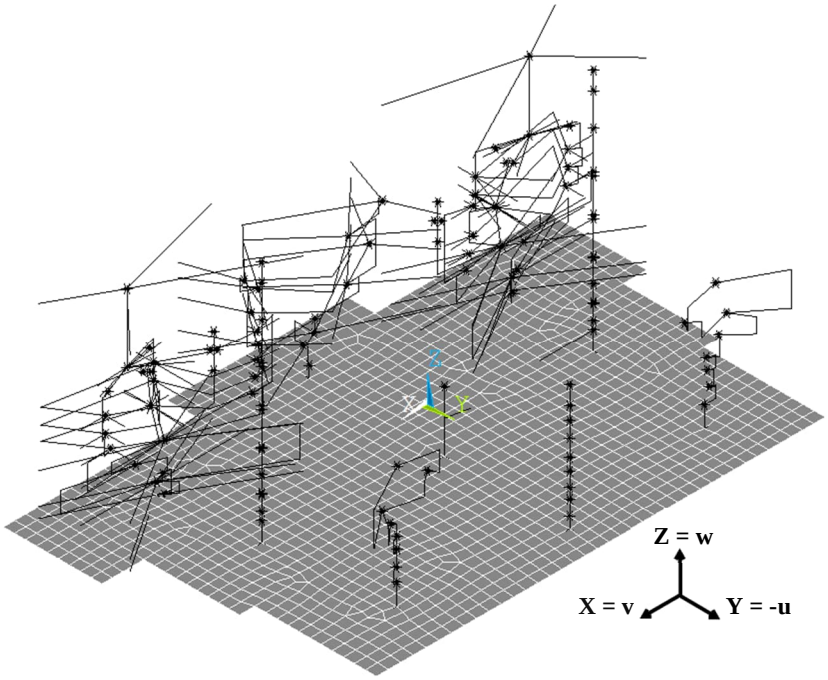

The local plant (u, v, z) and ANSYS (x, y, z) coordinate system

Figure 3. ANSYS FE model of the Cruas Nuclear Island (NI).

Accurate determination of the horizontal stiffness (K_h) of the bearings is crucial for predicting seismic response of the isolated structure. The horizontal stiffness depends on the shear modulus of the elastomer (G_d), the bearing area (A), and the total elastomeric thickness (h), and can be calculated as $K_h = G_d \times A/h$.

The benchmark organisers provided the ageing curve and the distortion test data for the elastomeric bearings. As shown in Figure 4, the shear modulus (G_d) increases with ageing by up to ca. 40% and decreases with lower distortion levels (γ), where $\gamma=\Delta x/h$, and Δx is the horizontal displacement of the bearing. Distortion test data were provided for the years: 1989, 1985, 1990 and 2008. The corresponding

ageing coefficients, defined as the ratio of the shear modulus at a given year to its value in 1979 (production year), are 1.02, 1.18, 1.26 and 1.38, respectively. An aging coefficient of 1.39 was determined for the shear modulus expected in 2019, the year of the Le Teil earthquake.

The maximum distortion γ during the "Le Teil" earthquake was only 6.5% (Δx = 2.6 mm). However, the available distortion test data covers only near-zero distortion values and large distortions exceeding 60% ($\Delta x \approx 24$ mm), making direct interpolation challenging (Figure 4). To estimate the shear modulus (G_d) at this intermediate strain level, a logarithmic curve fit was applied to the 2019 dataset. The resulting shear modulus at γ = 6.5 % is G_d = 2.53 MPa, leading to a total system stiffness (for 1812 bearings) of $K_{h,tot}$ = 28 230 MN/m. Using a SDOF approximation, the computed fundamental eigenfrequency of the system with a total mass M_{tot} = 366.2 Kt is f = 1.39 Hz. To match the target fundamental frequency ($f_0 \approx 1.5$ Hz) in both horizontal directions (u and v) from the Stage 1 modal analysis provided by the organizers, the shear modulus was increased to G_d = 3.05 MPa at γ = 6.5%). This adjustment results in a final system stiffness of $K_{h,tot}$ = 34 090 MN/m.

The compression stiffness of the bearing pads $K_{vert,}$ is determined using established formulas from the literature, yielding a total vertical stiffness of $K_{vert,tot}$ = 10 872 GN/m. Based on dynamic test data provided by the organizers, a damping ratio of ζ = 7% is assumed for the bearings in both the horizontal and vertical directions.

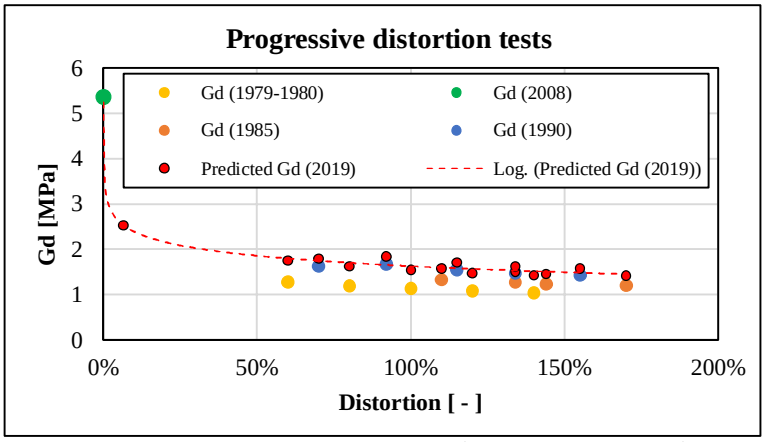

The dashed red line represents the logarithmic fit used to estimate G_d for 2019

Figure 4. Progressive distortion test data of elastomeric bearings from different years, showing the evolution of shear modulus G_d with increasing distortion.

In Stage 1 of Phase 3, the seismic bearings are modelled as linear springs in both horizontal and vertical directions, with horizontal stiffness $K_{h,tot,u}$ = $K_{h,tot,v}$ = 34 090 MN/m, vertical stiffness $K_{vert,tot}$ = 10 872 GN/m, and damping ratio ζ = 7%. However, post-processing of the recorded earthquake data following the completion of Stage 1 revealed directional variations in the system's horizontal fundamental frequencies: $f_u \approx$ 1.51 Hz ($\rightarrow K_{h,tot,u}$ = 33 100 MN/m) in the transverse direction (u), and $f_v \approx$ 1.68 Hz ($\rightarrow K_{h,tot,v}$ = 40 874 MN/m) in the longitudinal direction (v). These stiffness differences are primarily attributed to variation in displacement amplitudes between the two directions, leading to different distortion levels and stiffness values in the bearings. This finding highlights the importance of considering the nonlinear behaviour of elastomeric bearings for accurate predictions of the isolated system's response.

To address this, in Stage 2 a nonlinear elastic force-deflection relationship (Figure 5) is introduced in the ANSYS model, ensuring that stiffness variations with strain are accurately captured. A trilinear force-deflection curve is implemented, as shown in Figure 5. Since the maximum distortion during the earthquake

is significantly lower than the distortion levels for which shear modulus values are provided in the tests, the curve points are derived based on the following assumptions:

- for very low distortion values, an initial shear modulus of 5.5 N/mm^2 is assumed for displacements up to 0.5 mm.
- the next two points in the force deflection curve, at 1.5 mm and 2.1 mm correspond to the maximum deflections recorded during the Le-Teil earthquake in transverse (u) and longitudinal (v) directions, respectively.
- The corresponding forces at these points are computed to match the fundamental frequencies of 1.68 Hz and 1.51 Hz, ensuring consistency with the recorded seismic response.
- For displacements exceeding 1.5 mm, the tangent stiffness remains constant at $G_{d,tan}$ = 1.2 N/mm^2, as summarized in Table 1.

Two different damping models are implemented in the ANSYS. The superstructure stick models are assigned 2% Rayleigh damping, while the seismic bearings are modelled with a constant damping coefficient of C_{tot} = 472 423 $\frac{kN}{m}s$, corresponding to a damping ratio $\zeta \approx$ 5 - 7%. It is important to note that, since the introduced force-deflection curve is purely elastic, no kinematic hardening effects are considered in the model.

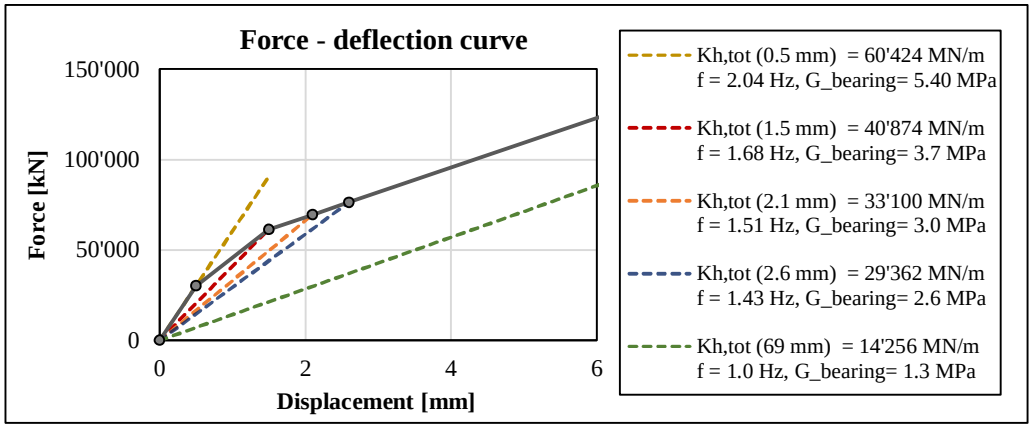

Figure 5. Calibrated force deflection curve used as input in the ANSYS Model for Calibration Phase 2. The secant stiffness values ($K_{h,tot}$) are derived at different displacement levels, corresponding to variations in fundamental frequency and shear modulus of the seismic bearings

Table 1. Key points of the force-deflection diagram implemented in ANSYS APDL

Distortion	Displacement	Force	Secant Stiffness	Tangential Stiffness	Secant Shear Modulus	Tangential Shear Modulus
γ	d	F	k_{sec}	k_{tang}	$G_{d,sec}$	$G_{d,tang}$
-	mm	kN	MN/m	MN/m	N/mm^2	N/mm^2
0%	0	0	-	-	-	-
1%	0.5	30'212	60'424	60'424	5.4	5.4
4%	1.5	61'311	40'874	31'100	3.7	2.8
5%	2.1	69'510	33'100	13'664	3.0	1.2
6%	2.6	76'342	29'362	13'664	2.6	1.2

NUMERICAL ANALYSES AND RESULTS

The following figures (Figure 6 – Figure 7 – Figure 8) present the calculation results from Stage 1 (ST1) – a blind prediction with linear model – and Stage 2 (ST2) – a calibrated model incorporating nonlinear bearing behaviour. These results are compared to the recorded data (REC) provided by the organisers after the completion of Stage 1. Figure 6 shows the results for the sensor EAU 001, Figure 7 for the sensor EAU 002 and Figure 8 for the sensor EAU 003, the sensor locations are described in Figure 2.

The modal analysis in Stage 1 (with constant stiffness of the bearings) resulted in fundamental frequencies of 1.45 Hz and 1.47 Hz in the two horizontal directions, with ca. 98% of the total mass participating in these modes. This confirms that, under the initial assumption of equal bearing stiffness in the two horizontal directions, the Nuclear Island (NI) behaves as a rigid body, exhibiting symmetric displacement in both horizontal directions.

The acceleration response spectra derived from the transient analysis in Stage 1 exhibit a peak at around 1.5 Hz at all three sensor locations. This peak corresponds to the rigid body motion of the stiff structures on the flexible seismic bearings. In contrast, at the fundamental frequencies of the buildings (starting from 4 Hz) and the soil resonance range (7 – 9 Hz), no significant peaks are observed. This suggests that the rigid-body response of the Nuclear Island (NI) dominates the seismic behaviour, as expected for a base isolated system. The limited response at higher frequencies (> 4 Hz for buildings, 7–9 Hz for soil) indicates that these effects are less pronounced in Stage 1, likely due to the simplified linear bearing model, which does not fully account for nonlinearities and soil-structure interaction (SSI) effects.

The Stage 1 (ST1) results show good agreement with the recorded data (REC), especially in terms of amplitudes near the first peak in the u-direction. However, in v direction, the recorded data reveal a frequency shift in the fundamental frequency of the structure, which is not captured in the Stage 1 calculation. This discrepancy suggests that the effective stiffness of the bearings differs between the u- and v- directions, likely due to unequal displacement amplitudes in each direction, leading to direction-dependent variations in bearing stiffness. Additionally, while the Stage 1 spectra (blue) do not exhibit significant peaks at the fundamental frequency of the soil (7 – 9 Hz), the recorded data from the sensors EAU 001 and 003 (located at the base of the buildings) show a clear peak in this frequency range. This indicates that soil-structure interaction (SSI) effects are more pronounced in the actual response than in the simplified Stage 1 model.

The implementation of the nonlinear force-displacement curve (ST2) significantly improves the acceleration spectra, particularly in the v-direction. ST2 not only captures the first peak at 1.5 Hz in v-direction more accurately, but it also provides a more realistic representation of spectral accelerations above 1.5 Hz, especially at sensors EAU 001 and EAU 003. However, the acceleration peak at the fundamental frequency of the soil (7 – 9 Hz) is slightly overestimated. Additionally, high-frequency peaks up to 10 Hz are better captured at the EAU-002 sensor location, indicating an overall improvement in modelling higher-frequency response components. Nevertheless, the amplification in the v-direction between 1.5 Hz and 2 Hz is overestimated which may be attributed to simplifications in the reactor building model, where sensor EAU-002 is located. Further refinements to the structural representation of the reactor building could help improve accuracy in this frequency range.

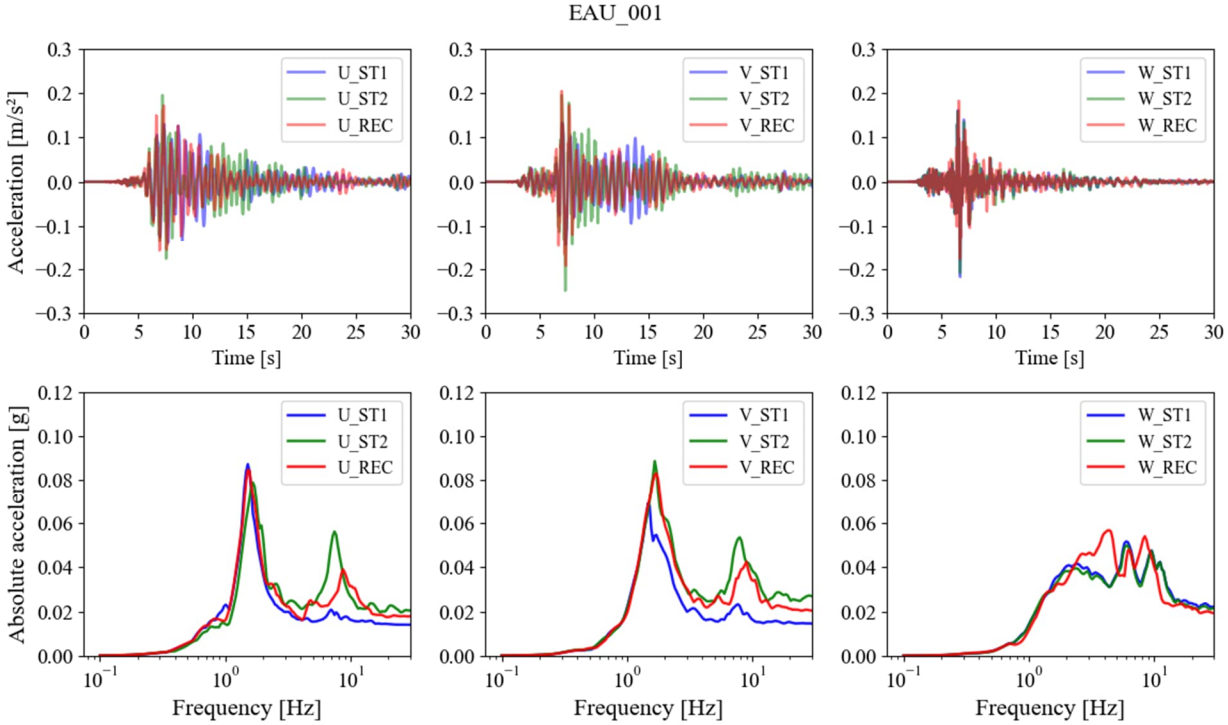

Figure 6. Acceleration time history (top) at sensor EAU_001 and corresponding response spectra (bottom) for damping ratio ζ = 5% in the u, v and w directions of the local coordinate system

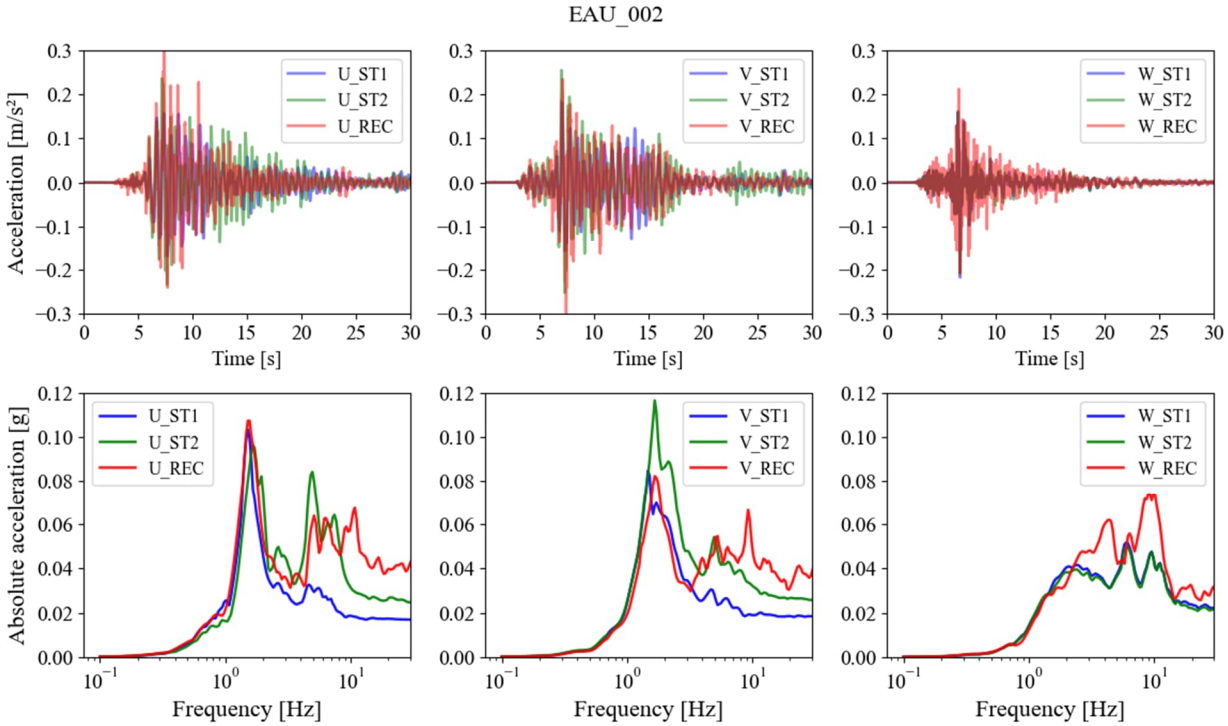

Figure 7. Acceleration time history (top) at sensor EAU_002 and corresponding response spectra (bottom) for damping ratio ζ = 5% in the u, v and w directions of the local coordinate system

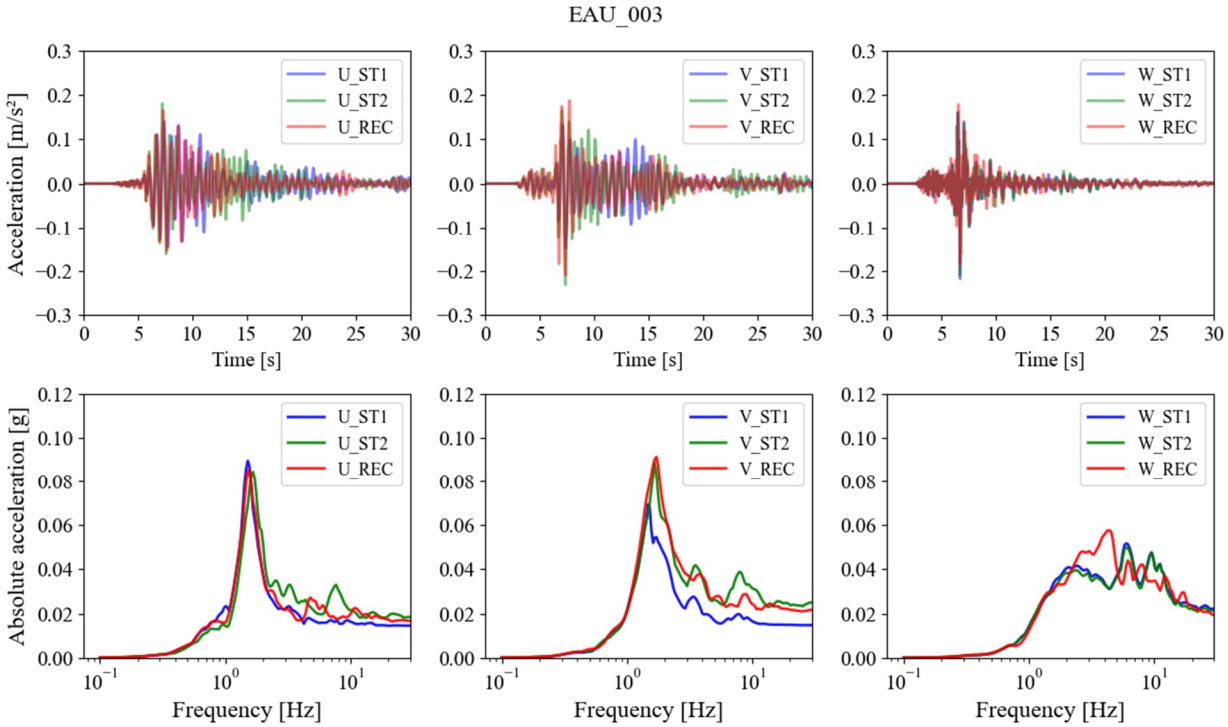

Figure 8. Acceleration time history (top) at sensor EAU_003 and corresponding response spectra (bottom) for damping ratio $\zeta = 5\%$ in the u, v and w directions of the local coordinate system

The differences in response spectra between the linear bearing model (ST1) and the nonlinear bearing model (ST2) can be attributed to variations in stiffness and damping behaviour. The high-frequency content of the Foundation Input Motion is primarily associated with small displacement amplitudes. In the nonlinear bearing model (ST2), at small displacements ($\Delta x < 0.5$ mm), the effective stiffness increases to $k_{eff} \approx 60\ 425$ MN/m, allowing for greater transmission of high-frequency vibrations to the structure and leading to higher acceleration amplitudes. In contrast, in the linear model (ST1), the bearing stiffness remains constant at $k_{eff} \approx 34\ 000$ MN/m, which results in stronger attenuation of high-frequency, small-amplitude vibrations due to the lower stiffness. At the same time, constant damping coefficient approach causes the damping ratio to decrease to approximately 5 % for high stiffness values and small displacements, reducing energy dissipation at high frequencies. As a result, the multi-linear force-displacement behaviour in ST2 more accurately captures the stiffness variations of the bearings with displacement, leading to a closer match with the recorded response spectra.

As demonstrated by the time-frequency plots of the acceleration time-histories in Figure 9 and Figure 10, obtained using the Stockwell wavelet transform (ST), the inclusion of nonlinear springs enhances the capture of higher-frequency content. The fundamental frequency, ranging between 1.4 Hz and 1.7 Hz, remains dominant throughout the entire earthquake duration, with high acceleration amplitudes observed between 5 and 10 s. At sensor EAU 001, the high-frequency content is predominantly present between 5 s and 10 s in both the recorded data and the Stage 2 calculation, indicating good agreement. At sensor EAU 002, however, high-frequency vibrations persist in the recorded data until approximately 20 seconds, whereas in the Stage 2 calculation, they diminish after 10 seconds. Additionally, frequencies exceeding 10 Hz, which appear in the recorded data at EAU 002, are not captured in the calculated results. This discrepancy is likely due to the simplified building model, which does not account for secondary eigenmodes that contribute to the response at these frequencies.

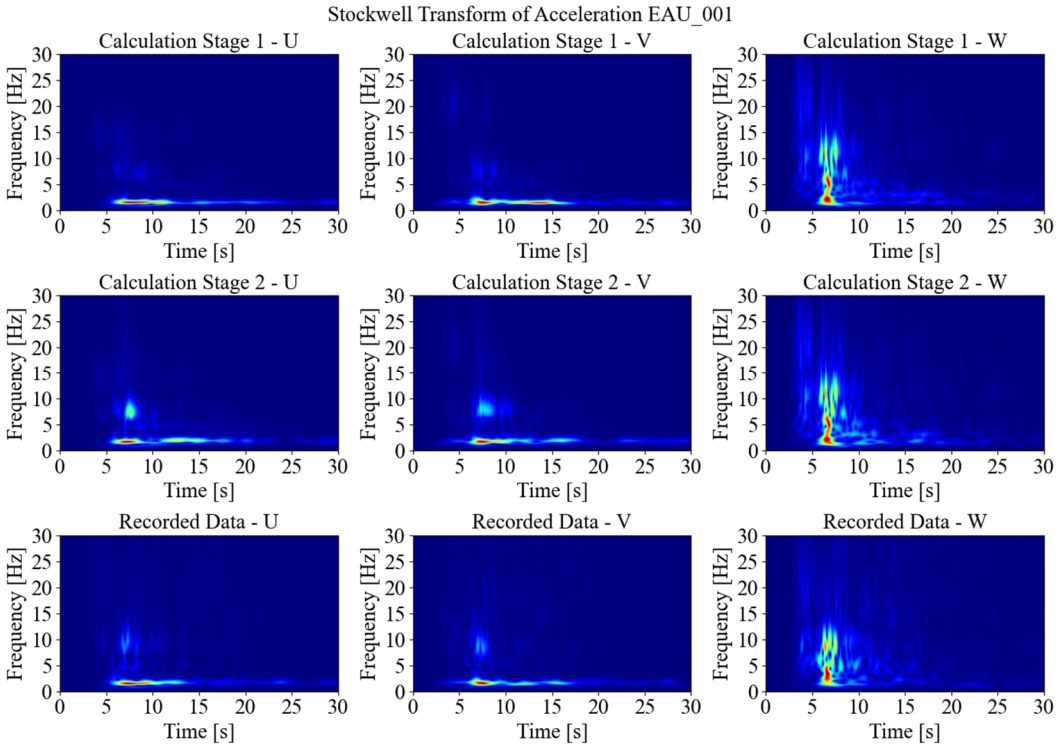

Figure 9. Time-frequency plots of acceleration at sensor EAU_001 in the u, v, and w directions obtained using the Stockwell wavelet transform (ST)

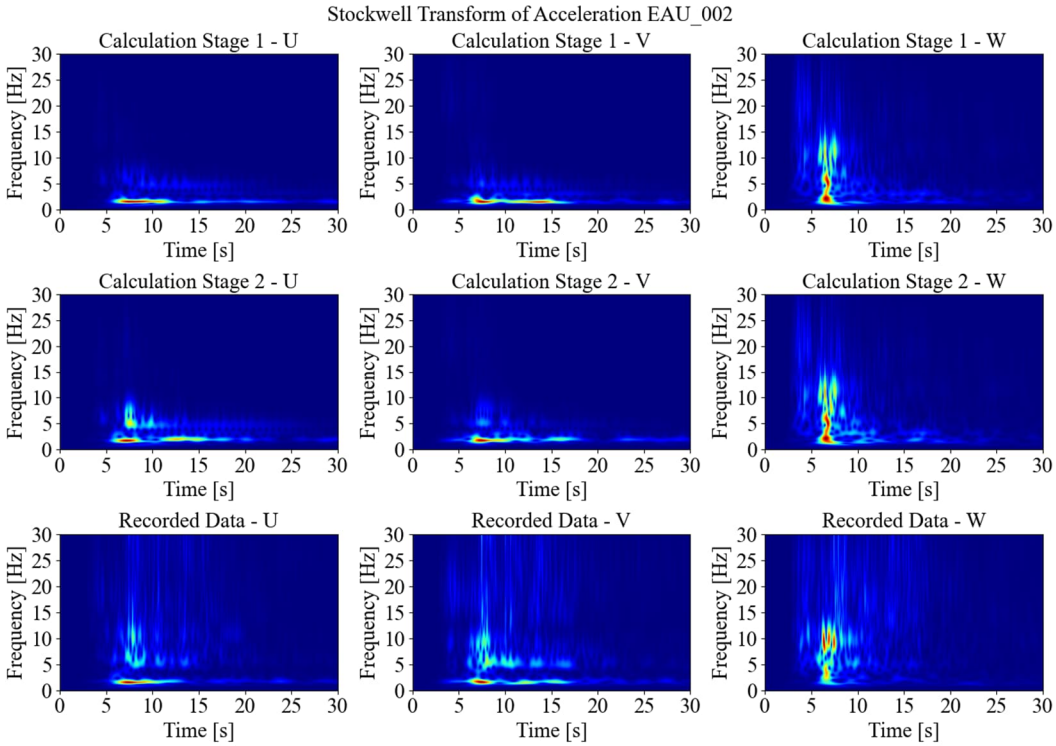

Figure 10. Time-frequency plots of acceleration at sensor EAU_002 in the u, v, and w directions obtained using the Stockwell wavelet transform (ST)

CONCLUSION

This paper reports on the modelling and the seismic response analysis of the base-isolated Cruas NPP subjected to the Le-Teil earthquake within the international benchmark SMATCH. It has been shown that accurately modelling the realistic, nonlinear behaviour of the seismic bearings is crucial for capturing the response of the structure at small earthquake displacements. The good agreement between the SMATCH benchmark Stage 2 results and the recorded data at sensors EAU 001 and EAU 003, located near the upper raft, indicates that the isolator bearing characteristics – specifically stiffness and damping – are realistically represented in the model. However, a comparison with sensor EAU 002, located higher in the reactor building, reveals that certain spectral peaks are not adequately captured. These discrepancies may arise from simplifications in the superstructure model, which neglect local mode shapes.

The analysis demonstrates that simplified superstructure modelling using stick models effectively captures the global response of the Nuclear Island while significantly reducing computational time. However, for a more detailed assessment of individual building components, a refined superstructure model is recommended to better capture local mode shapes. Given the good fit of the calculated and recorded accelerations, detailed soil-structure interaction modelling appears to be less critical for the global horizontal response of base-isolated structures founded on a stiff soil stratum. However, this conclusion may not be directly transferable to all site conditions and isolation device configurations.

REFERENCES

Ansys Academic Research Mechanical APDL, Release 2021 R2.

EDF/IRSN/Egis: SMATCH Benchmark, Seismic Base Isolated Nuclear Power Plant Shaken by a Real Earthquake, https://smatch-benchmark.org/.

Viallet, E., Berger, J., Traversa, P., El Haber, E., Hervé-Secourgeon, E., Hervé-Secourgeon, G., Zuchowski, L., and Dupuy, G. (2022). “2019-11-11 Le Teil Earthquake - The ultimate missing piece of experience feedback related to a nuclear power plant built on seismic base isolation: A real earthquake”, SMiRT-26, Berlin/Potsdam, Germany